JMB

Available online at www.sciencedirect.com

SCIENCE DIRECT°

ELSEVIER

Secondary Structure of α-Synuclein Oligomers: Characterization by Raman and Atomic Force Microscopy

Mihaela M. Apetri[1], Nakul C. Maiti[2], Michael G. Zagorski[1], Paul R. Carey[1,2] and Vernon E. Anderson[1,2]*

[1]*Department of Chemistry, Case Western Reserve University, Cleveland, OH 44106, USA*

[2]*Department of Biochemistry Case Western Reserve University, Cleveland OH 44106, USA*

Formation of α-synuclein aggregates is proposed to be a crucial event in the pathogenesis of Parkinson's disease. Large soluble oligomeric species are observed as probable intermediates during fibril formation and these, or related aggregates, may constitute the toxic element that triggers neurodegeneration. Unfortunately, there is a paucity of information regarding the structure and composition of these oligomers. Here, the morphology and the conformational characteristics of the oligomers and filaments are investigated by a combined atomic force microscopy (AFM) and Raman microscopic approach on a common mica surface. AFM showed that *in vitro* early stage oligomers were globular with variable heights, while prolonged incubation caused the oligomers to become elongated as protofilaments. The height of the subsequently formed α-synuclein filaments was similar to that of the protofilaments. Analysis of the Raman amide I band profiles of the different α-synuclein oligomers establishes that the spheroidal oligomers contain a significant amount of α-helical secondary structure (47%), which decreases to about 37% in protofilaments. At the same time, when protofilaments form, β-sheet structure increases to about 54% from the ∼29% observed in spheroidal oligomers. Upon filament formation, the major conformation is β-sheet (66%), confirmed by narrowing of the amide I band and the profile maximum shifting to 1667 cm^{-1}. The accumulation of spheroidal oligomers of increasing size but unchanged vibrational spectra during the fibrillization process suggests that a cooperative conformational change may contribute to the kinetic control of fibrillization.

© 2005 Elsevier Ltd. All rights reserved.

Keywords: α-synuclein; oligomers; secondary structure; Raman microscopy; protofibrils

*Corresponding author

Introduction

Neuronal loss and accumulation of intracellular or extracellular protein aggregates are common characteristics of a wide variety of neurodegenerative diseases.[1] On the basis of several observations, α-synuclein aggregation is thought to have an important role in Parkinson's disease (PD): (1) α-synuclein was found to be a major fibrillar component of Lewy bodies and Lewy neurites, intracytoplasmic inclusions that are the neuropathological hallmark of PD;[2] (2) two mutations in the α-synuclein gene (A53T and A30P) have been linked to early onset of PD;[3,4] and (3) the overexpression of this protein in both mice and Drosophila has been shown to lead to PD-like phenotypes typified by motor deficits and neuronal loss.[5,6] *In vitro*, α-synuclein fibrillization is not a simple two-state transition from monomer to fibrils, but rather a complex process that involves oligomeric intermediates of various sizes and morphologies. These oligomers are heterogeneous and are, moreover, transient, since they are consumed as fibrillization proceeds.[7–11] Several studies have suggested that the prefibrillar oligomers, rather

than the mature fibrils, could be pathogenic.[5,8,12] Thus, there are distinct steps in the aggregation process where intervention might be able to prevent or reverse the formation of oligomers and/or fibrils. While the conformational analysis of the protein at different states of aggregation is vital for understanding the mechanism of fibril formation and for potentially developing effective therapeutics, very little is known about the structures of these intermediates.

The conformational states of α-synuclein at the beginning and end stages of the fibrillization process are better characterized. Our previous Raman data of monomeric α-synuclein in aqueous solution suggest that the peptide bonds are distributed in both α-helical and extended β-regions,[13] consistent with the NMR observations of N-terminal residues with α-helical propensity.[14] During α-synuclein fibril formation, the protein undergoes a conformational change[7,15] and, on the basis of X-ray and electron diffraction studies, α-synuclein assemblies adopt a cross-β conformation with individual β-strands perpendicular to the fiber.[16]

The structure and composition of the oligomeric aggregates observed as intermediates during fibril formation remain ill-defined, due to the inability to use high-resolution techniques. Neither NMR spectroscopy nor X-ray crystallography can be used, since the spheroidal oligomers are transient species that are large and inherently non-crystalline. However, some information on the secondary structure has been gained from circular dichroism (CD) studies.[9,12] Raman spectroscopy may represent a more powerful approach in this area, since it is capable of providing structural information of proteins in various states: aqueous solutions,[13,17] insoluble aggregates,[18,19] fibrils and crystals.[20,21] Analysis of protein amide I band profiles provides information on secondary structure, and the Raman spectra furnish several sensitive markers of side-chain orientation, environment and interactions.[21,22] The feasibility of the method is not hindered either by the size of the supramolecular assembly or by light-scattering artifacts that can severely restrict the use of other spectroscopic probes. The conformation of α-synuclein, in particular, has been characterized by Raman
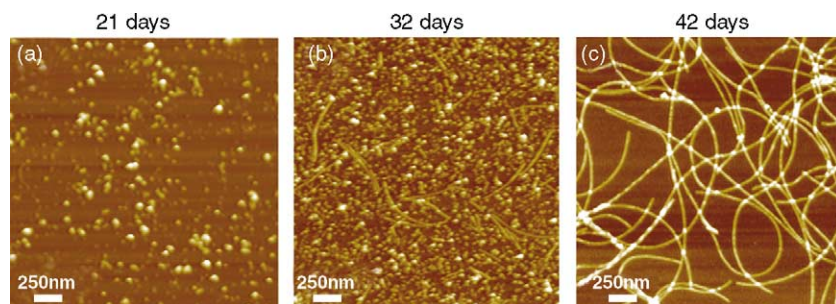
spectroscopy, as small additions of methanol enhance β-sheet formation and hexafluoro-isopropanol induces almost complete conversion to α-helix.[13]

Here, we use Raman microscopy to investigate in greater detail the secondary structural changes that occur during α-synuclein aggregation. The changes in secondary structure are correlated with the changes in the morphology of the aggregates visualized by atomic force microscopy (AFM). AFM is an ideal tool to correlate the stages of protein aggregation with Raman microscopy, because it is capable of directly detecting and characterizing the morphology of all α-synuclein aggregates present, from small intermediate oligomers to the final fibrils,[7,23,24] and it utilizes the same mica substrate.
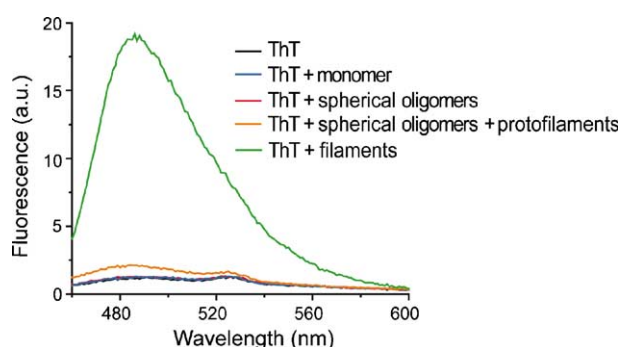
Results

AFM morphological studies of the α-synuclein aggregates

Distinct morphologies of the *in vitro* formed α-synuclein aggregates have been reported: non-fibrillar oligomers (protofibrils) such as spheres (2–6 nm in height), chains of spheres (∼4 nm in height) and rings (3–7 nm in height) and fibrillar species such as filaments (∼5 nm in height) and fibrils (8–10 nm in height).[10,24–26] The morphology of the oligomers can be affected by the solution conditions, including the presence of lipids[27–29] or metal ions.[30] Figure 1 shows AFM images of different species formed during α-synuclein aggregation. The height or *z*-dimension was used to estimate the diameters of the different aggregates, since the *z*-dimension is generally more accurate and is not affected by the "tip-broadening" effect.[31] The ranges for the heights were determined by measuring more than 50 cross-sectional height profiles of each species. Incubation of freshly prepared monomeric α-synuclein (300 μM) solution at 37 °C, without agitation for several weeks, was monitored by removing aliquots at different time-points, removing monomeric α-synuclein and allowing the protein aggregates to adsorb onto a mica surface for analysis by AFM. After 21 days of

Figure 1. AFM images (2.5 μm × 2.5 μm) of α-synuclein in different aggregates: (a) spheroidal oligomers after 21 days of incubation; (b) spheroidal oligomers and protofilaments after 32 days of incubation; and (c) filaments after 42 days of incubation. Aliquots have been taken from 300 μM aged protein solutions and the α-synuclein aggregates were separated from monomeric protein and concentrated as described in Materials and Methods. The images were recorded immediately at room temperature (23 °C). The Z-range for all AFM images was 20 nm.
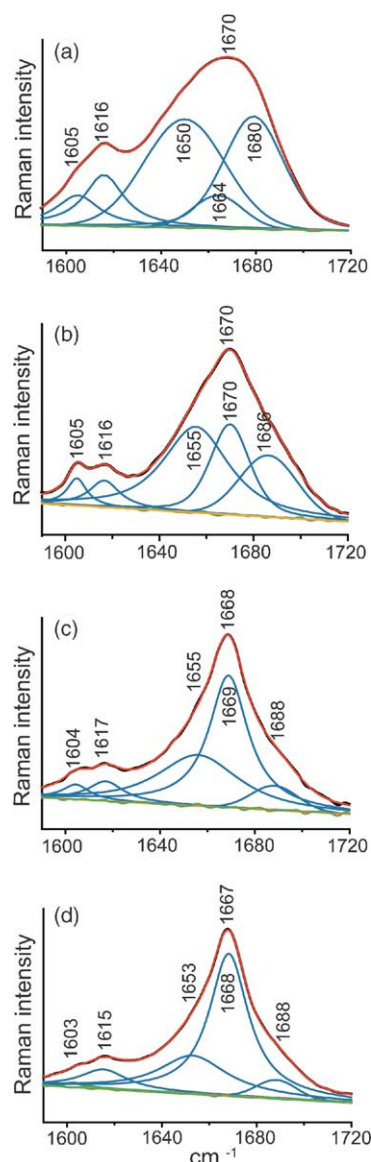
Figure 2. Fluorescence spectra of ThT alone and mixed with the separated α-synuclein aggregates. There is essentially no ThT fluorescence enhancement upon addition of oligomeric material, but there is a slight increase in ThT fluorescence when the protofilaments were present.

incubation the first formed α-synuclein aggregates observed by AFM were the spheroidal oligomers (Figure 1(a)). Based on their height differences, smaller (1.4–3.5 nm) and larger (4.0–7.5 nm) spheroidal oligomers were detected. After 11 more days of incubation, elongated aggregates (chain of spheres, referred to here as protofilaments) with heights of ~5 nm were seen along with the spheroidal oligomers (Figure 1(b)). The final α-synuclein filaments (4.5–6.0 nm in height) seen by AFM after 42 days of incubation (Figure 1(c)) appear to be elongations of this species. Previously, such filaments (height ~5 nm) have been reported from *in vitro* studies,[7,24] and similar structures have been isolated from PD-affected brains.[2] The changes in thioflavin-T (ThT) fluorescence upon addition of the separated aggregates are shown in Figure 2. ThT emission spectra of the monomer and spheroidal oligomers are effectively identical, suggesting that these aggregates, in common with the monomer, do not enhance the fluorescence of ThT, consistent with an absence of the crossed β-sheet structure common to amyloid fibrils. However, a slight increase in the ThT fluorescence was observed when the proto-filaments are formed and a much larger fluorescence (over tenfold greater) enhancement is observed in the presence of α-synuclein filaments.

Conformational characteristics of the separated α-synuclein aggregates

The same separated species formed during the aggregation of α-synuclein and analyzed by AFM were adsorbed onto a smooth mica surface and were subjected to analysis by Raman microscopy. A band-fitting approach[13] based on the Raman spectra of α-synuclein converted quantitatively either to α-helix (1650–1655 cm^{-1}), β-sheet (1664–1670 cm^{-1}) or extended β-strand and polyproline II (PPII) structure (1671–1680 cm^{-1}), was employed to identify the presence, or change in the relative

contribution of the secondary structural elements. Figure 3 shows the deconvolutions of the Raman amide I bands of α-synuclein in the different aggregates. Two bands, at 1604 cm^{-1} and 1615 cm^{-1}, attributed to the ring modes of the Phe and Tyr residues, are included in the band-fitting protocol. During α-synuclein aggregation, the Raman amide I band narrows dramatically and the peak maximum decreases from 1670 cm^{-1} to 1667 cm^{-1}, consistent with a progressive increase

Figure 3. Amide I region (1590–1720 cm^{-1}) of the Raman spectra of separated α-synuclein aggregates. The amide I regions of α-synuclein as (a) monomer in solution, (b) spheroidal oligomers on mica, (c) spheroidal oligomers with protofilaments on mica and (d) filaments on mica were fitted into three component amide I bands. Two bands at ~1604 cm^{-1} and ~1615 cm^{-1}, assigned to the aromatic residues Phe and Tyr were included along with the amide I bands in the fitting procedure. The black line is the original spectrum, blue lines are the individual component bands and the red line is the sum of the bands. Baseline (orange) and residuals of the fit (green) are shown.

Table 1. Band fitting of the amide I band profile of different α-synuclein species

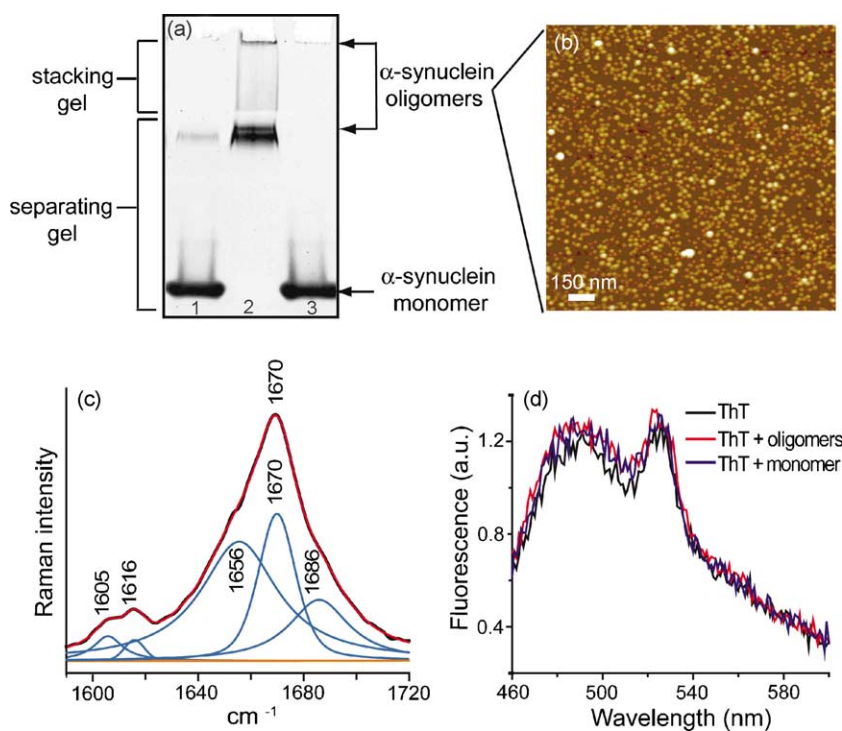| Peak no.	Center (cm^{-1})	Width (nm)	% Area
Monomer			
1	1650	40	49
2	1664	25	10
3	1680	30	41
Spheroidal oligomers			
1	1655	33	47
2	1670	20	29
3	1686	28	24
Spheroidal oligomers + protofilaments			
1	1655	40	37
2	1669	22	54
3	1688	20	9
Filaments			
1	1653	34	28
2	1668	31	66
3	1688	35	6

in β-sheet structure occurring with the formation of more ordered aggregates. The amide I band at $1667\,cm^{-1}$ is a marker for β-sheet structures and is the characteristic feature observed in other amyloid fibrils.[13,18,19,32]

An advantage of the band-fitting technique is that it permits a quantitative estimation of the component bands in a spectrum. The integrated areas from the band-fitting procedure are given in Table 1. The fit of the amide I peak ($1590–1720\,cm^{-1}$) of α-synuclein monomer in solution shows that the major intensity (49%) is found in the component band at $1650\,cm^{-1}$, which is a marker for α-helical conformation, 41% of the amide I band intensity is extended-β and PPII structure, and the remaining intensity is assigned to β-sheet conformation. Comparison of the α-synuclein monomer with the spheroidal oligomers shows that the oligomers preserve their α-helical content

to ∼47%, while an increase from 10% to 29% β-sheet is observed with a concomitant decrease from 41% to 24% of extended and PPII structure (with the formation of protofilaments, a slight decrease in α-helical content (37%) is seen, while the extended and PPII structure decreases to 9%). Because the protofilaments are not completely separated from the spheroidal oligomers, the changes detected indicate only the direction of the conformational change that occurs and not the full extent of the change. In the fibrillar state, the major conformation is β-sheet (66%). While the accuracy of the assignment of the secondary structural composition is prone to some error,[33] the changes in the amide I band demonstrate unequivocal changes in conformation and increases in β-sheet with a compensating decrease in α-helical conformation as the oligomers adapt to a more uniform structure in the protofilaments and fibrils.

Characterization of spheroidal oligomers produced upon solubilization of lyophilized α-synuclein

Another method to produce spheroidal oligomers is by solubilization of lyophilized α-synuclein. These aggregates were separated from monomeric protein in the same way as the oligomers formed by extended incubation. These oligomers before and after centrifugal filtration were loaded onto a non-denaturing polyacrylamide gel (Figure 4(a)) to verify the separation. The analysis of the separated oligomers by AFM showed the presence of a compact population of smaller spheroidal oligomers (1.5–3.2 nm in height) and a small number of larger aggregates (3.9–7.0 nm) (Figure 4(b)). The fits

Figure 4. Spheroidal oligomers formed upon solubilization of the lyophilized α-synuclein as monitored by native PAGE, AFM, Raman microscopy and ThT. (a) In the native polyacrylamide gel, the lyophilized α-synuclein (1) before filtration through a Microcon 100 kDa cutoff centrifugal filter, (2) the retentate (oligomeric α-synuclein) and (3) the filtrate (monomer) are shown. (b) The AFM image (1.5 μm × 1.5 μm), (c) the amide I region of the Raman spectrum and (d) the ThT fluorescence spectra demonstrate the presence of spheroidal oligomers with morphologies and conformational features similar to those of the oligomers formed by extended incubation of α-synuclein. The band-fitting protocol is the same as that used for Figure 3.

of the amide I peak of α-synuclein oligomers prepared according to the two protocols were nearly identical (Figures 3(b) and 4(c)); the only quantitative difference being that the amide I band for the oligomers produced from lyophilized sample (Figure 4(c)) is narrower, the bandwidth at half-height being 34 cm^{-1} compared to 37 cm^{-1} for the oligomers formed slowly from monomer. The difference may reflect the presence of a more homogeneous population of aggregates. Neither preparation of spheroidal oligomers enhances the fluorescence of ThT (Figure 4(d)). Thus, the spheroidal oligomers prepared according to the two protocols have similar morphologies and conformational features.

Discussion

Raman spectroscopy and Raman microscopy have the potential to provide secondary structural information of proteins in various states: as soluble monomers[13] as well as insoluble fibrillar aggregates.[18,19,32] The information regarding the protein secondary structure is reflected in the Raman amide I band region (1640–1690 cm^{-1}) and the amide III band region (1230–1300 cm^{-1}).[34,35] Recently, we developed a quantitative estimate of the secondary structure of natively unfolded proteins based on a three-component band-fitting of Raman amide I band, since the analysis of amide III band is complicated by overlapping bands from side-chain vibrations.[13] Raman microscopy, when compared to other spectroscopic techniques, has the unique advantage of not being restricted by the size of the assembly or by light-scattering artifacts that can mask the spectra. More recently, our laboratory utilized Raman microscopy to characterize the structure of amyloid-β peptide present in the senile plaque cores isolated from human autopsy tissue.[18] Thus, this method is an appropriate tool to structurally characterize aggregates formed during protein fibrillization processes. *In vitro* studies can support subsequent analysis of *ex vivo* samples.

In vitro α-synuclein aggregation studies have revealed the formation of soluble oligomeric intermediates, characterized occasionally as protofibrils, which disappear upon fibril formation. The earliest formed α-synuclein non-fibrillar aggregates appear to be spheroidal with heights between 2 nm and 6 nm.[8,12,25,26] Despite the importance of α-synuclein aggregation in PD, the identity of the pathogenic species and mechanism of toxicity are uncertain. Lansbury *et al.* have suggested that the non-fibrillar aggregates rather than the mature fibrils could be responsible for cell death in PD.[12,36] Thus, characterization of the structure of these intermediate oligomers may be crucial to designing novel therapeutic strategies to prevent formation of the oligomer and in deciphering the mechanism of toxicity.

In order to describe the conformational changes during α-synuclein aggregation in more detail, we analyzed the aggregates formed *in vitro* using the combination of Raman microscopy and AFM. In this way, we were able to get structural information as well as the morphological features of the aggregates observed during fibril formation. A particular advantage of our approach is that in both methods the aggregates were adsorbed onto the same substrate, the mica surface, assuring that both analyses were of the same form of α-synuclein. The single difference in sample treatment is that the protein-coated mica surface is washed prior to AFM, but simply allowed to dry for the Raman study. This procedure may selectively remove an intermediate form with minimal affinity for the mica surface. The isolation process successfully eliminated contamination of the oligomers and protofilaments by both monomer and fibrils. However it has proven difficult to completely separate protofilaments formed in aqueous solution from the spheroidal oligomers.

Structural characterization of amyloid fibrils formed from diverse proteins has largely been carried out on assemblies either formed *in vitro* or present in extracellular deposits.[37] X-ray fiber diffraction analyses of these fibrils revealed the presence of a common cross-β structure with β-strands perpendicular to the fibril axis and backbone hydrogen bonds parallel with the fibril axis.[16,38,39] Fourier transform infrared and solid-state NMR studies demonstrated that both parallel and antiparallel β-sheet orientations are present in the amyloid fibrils.[15,40–42]

While continuing progress has been made characterizing the structure of amyloid fibrils by solid-state NMR,[43–45] there is a lack of structural information regarding the intermediates formed during fibrillization. Teplow and co-workers believe that the formation of oligomeric intermediates containing significant amounts of α-helix are a key step in Aβ fibrillogenesis, and that during fibril formation a significant α-helix to β-structure conversion occurs.[46] A large spheroidal Aβ oligomer, termed a beta-ball, has been characterized by far-UV CD to 210 nm to contain β-structure.[47] Analysis of large oligomers by far UV-CD is complicated by the severe light-scattering necessarily associated with the large oligomeric structure. β-2 Microglobulin oligomeric intermediates are native-like in structure as determined by ^{1}H NMR and near-UV CD studies.[48] On the other hand, the Lansbury group, on the basis of far-UV CD studies, believes that spheroidal α-synuclein oligomers are rich in β-sheet structure and that the conversion from monomer to oligomers involves a secondary structural transition from natively unfolded to predominantly β-sheet.[9]

Our data reveal that the spheroidal oligomers formed by extended incubation or formed upon solubilization of the lyophilized protein retain a significant amount (47%) of α-helix and similar percentages of extended (24%) and β-sheet (29%)

structures. A significant extended to β-structure conversion and a slight α-helix to β-structure transition occur when the elongated oligomers (protofilaments) are formed. Because the protofilaments could not be separated completely from the spheroidal oligomers, only the direction of the structural change could be determined. During the formation of α-synuclein filaments, the α-helical content is reduced significantly (28%) and the proportion of β-sheet structure increases (66%), while the contribution of extended and PPII structure is minimal.

These secondary structural data demonstrate that, on aggregating into oligomers under physiological conditions, a significant change in the ensemble of structures present takes place; β-sheet structure is enhanced and the disordered or PPII secondary structure is diminished. Importantly, a significant proportion of the backbone torsion angles of the oligomeric α-synuclein remain in α-helical space in the spheroidal oligomers. In polypeptide sequences that lack regular secondary structure, the Raman spectrum is largely sensitive to the Ψ_n and Φ_{n+1} that border the amide bond, resulting in the potential for isolated residues in the α-helical region of Ramachandran space to contribute to the α-helical signal,[49,50] unlike CD, which requires the formation of a complete helical turn to generate an α-helical contribution to the spectrum. NMR studies have indicated that the N-terminal region has a propensity to be present in α-helical conformation, both in solution and in the presence of lipids.[14,51,52] The retention of α-helical character in these large oligomers is consistent with the observations that solvent conditions that favor partial α-helical formation enhance the aggregation of α-synuclein.[9,28,29,51] Since there is a significant increase in β-sheet structure in the oligomers, it suggests that the H-bonding present in the β-sheet contributes to the stabilization of the oligomeric structure. This H-bonding could be either inter- or intramolecular.

A complete secondary structural characterization of an unstructured protein in solution or in oligomeric form would require determination of the propensity of each residue to adopt a given conformation along with the degree of correlation between residues. Vibrational spectroscopy has the potential by isotope editing to characterize the contribution of individual residues[53] and, in favorable cases, of the correlation between residues in β-sheets.[54–56]

Our data are consistent with observations made by many others working on a variety of amyloidogenic systems: under all conditions examined, the spheroidal oligomers are formed prior to the appearance of fibrils and disappear as fibril formation reaches completion. The sequential nature of these events has led to the presumption that the oligomers are obligate intermediates in the fibrillization pathway.[28] (These common time-courses are equally consistent with an off-pathway equilibrium formation of the oligomers and/or

protofibrils. Establishing that any specific oligomeric form is an obligate intermediate in fibril formation is a difficult task.) If these oligomers are obligate intermediates, their conversion to the final fibril form is a critical step in the kinetics of fibrillization. We propose that the conversion of the oligomer to the cross-β structure present in the fibrils requires a cooperative conformational change. The cooperative nature of the change is consistent with the absence of any ThT fluorescence enhancement prior to the appearance of fibrils. The absence of ThT fluorescence enhancement in spite of the presence of β-sheet structure in the spheroidal oligomers suggests that the β-sheet is present in the core of the oligomers, or that the distinguishing feature of fibrils that results in the affinity and altered fluorescence properties is not present in the α-synuclein oligomers. The consistency of the Raman spectra of the spheroidal oligomers, independent of their size distribution, supports the proposal that a substantive conformational change occurs on protofilament and fibril formation from the spheroidal oligomer. This cooperative change in conformation can be likened to phase transitions observed in lipid bilayers, e.g. between bilayers and hexagonal phases.[57] Further characterization of the structure of the oligomeric intermediate(s) should permit the rational design of molecules that either stabilize the oligomeric intermediate and prevent fibrillization or promote the conversion of the oligomers to fibrils, a potentially less toxic form.

Materials and Methods

In vitro sample preparation for aggregation studies

Recombinant α-synuclein was expressed and purified as described.[13] The purified protein was dialyzed against deionized distilled water and lyophilized for storage at −80 °C. Lyophilization from buffer resulted in artificial formation of non-dissociable tetramer. Samples for aggregation studies were prepared by dissolving the protein in 20 mM sodium phosphate buffer (pH 7.5), containing 0.03% (w/v) sodium azide, followed by centrifugal filtration through a Microcon 100 kDa cutoff filter (Millipore). Protein concentrations were approximately 300 µM, as determined by UV absorbance measurements using an estimated extinction coefficient of 5800 M^{-1} cm^{-1} at 276 nm. Samples were incubated at 37 °C without agitation and the aggregation was followed by AFM using aliquots withdrawn at different time-points of incubation.

Separation of α-synuclein aggregates

The spheroidal oligomers were formed in two ways: slowly from incubation of the monomer (300 µM), and a larger fraction by solubilization of the lyophilized protein. For both methods, the aggregates were separated from monomer using a Millipore Microcon 100 kDa cutoff filter. The oligomeric α-synuclein was retained, while the monomeric protein passed through the filter, as verified by native polyacrylamide gel electrophoresis. The oligomers were recovered by gentle washing of the filter membrane with a 0.25 volume of buffer. The α-synuclein

filaments and fibrils formed after weeks of aging of the monomeric protein were isolated by centrifugation (16,000*g*) for 30 min and the pellet was gently resuspended in buffer.

Raman spectroscopy

Raman spectra of monomeric α-synuclein in solution were recorded using 647.1 nm Kr$^+$ laser excitation with 90° excitation/collection geometry and a Holospec f/1.4 axial transmission spectrometer (Kaiser Optical Systems, Inc.) employed as a single monochromator.[13,58] A back-illuminated charge-coupled device (CCD) from Princeton Instruments, Inc. was utilized as the detector. Synuclein (50–75 µl at a concentration of 300 µM) in 20 mM phosphate buffer (pH 7.5), was held in a 2 mm×2 mm quartz cuvette. Data were acquired using 0.8 W of laser power with spectral acquisition times of 5 min.

Raman spectra of α-synuclein in the different aggregated forms were recorded with the help of a Raman microscope system, as described.[18] The different α-synuclein species (30 µl) were applied onto freshly cleaved mica surfaces and air-dried. The aggregates were viewed *via* a long focal length objective and a video CCD camera was used for optical imaging. A standard illuminating light source (halogen lamp) was used for imaging and focusing the laser beam on the sample. The beam position was adjusted by viewing the video images on a computer monitor. Back-scattered light from the focal spot was collected by the same objective lens and the scattered light reached the Raman spectrograph through an optical filter and *via* a second optical fiber. The illuminating light source remained shut down during the Raman collection. The microscope was operated in the non-confocal mode to maximize light throughput: 50 mW of 647.1 nm laser excitation from a krypton laser was focused through the microscope using a 100× objective to generate the Raman scattering and the data acquisition time was 1–2 min. The focal volume was typically 5 µm in diameter and 25 µm in depth. The background and mica spectra were subtracted from the sample spectra. Spectra displayed in the Figures were averages of more than three individual spectra. Prior to recording a Raman spectrum, the frequency and the intensity axes were calibrated using neon light.

Mica is widely used as a substrate for AFM. An ideal substrate for AFM and Raman microscopy will absorb proteins on its surface with sufficient strength to retain the protein, but the interactions should not disrupt or alter the structure of the protein. The hydrophilic character of the mica surface has routinely met these requirements, and the more hydrophobic substrate graphite did not retain the oligomeric α-synuclein. For use as a substrate in Raman microscopy, the Raman spectrum of the surface should not have bands that interfere with the region of interest, and muscovite mica lacks any Raman feature above 1200 cm^{-1} providing a convenient spectral window for the amide I and III bands.

Band fitting of the amide I spectrum

Different amide mode vibrations of protein, which together constitute the amide I band, appear in the 1610–1720 cm^{-1} region of the Raman spectrum. The amide I band profile of proteins is a function of the secondary structure of the protein. α-Synuclein exhibits asymmetrical narrow, ∼25 cm^{-1} bandwidth at half-height, when solvent conditions result in the presence of solely β-sheet or α-helix. In the presence of hexafluoro-isopropanol, the α-helical structure has an amide I band at 1653 cm^{-1}, while in the presence of methanol or in fibrils, the β-sheet structure amide I band appears at 1667 cm^{-1}.[13] For random structure proteins, the amide I band appears in a region of higher frequency (1676–1690 cm^{-1}). As well as these bands, proteins show some weak coupling mode vibrations throughout the region. The presence of a mixture of secondary structural components results in a broad and asymmetric amide I band.

Conformational analysis of different α-synuclein aggregation states was performed by analyzing the asymmetric amide I bands in the Raman spectra. The amide I band (1590–1720 cm^{-1}) was fit with the CurveFit.Ab routine of GRAMS/32 which is based on the Levenberg–Marquardt non-linear least-squares method.[59] The band was fit assuming three symmetrical component bands that represent the different structural conformations that α-synuclein can adopt: α-helix (1653 cm^{-1}), β-sheet (1667 cm^{-1}), and extended β-strand and PPII structure (1674–1685 cm^{-1}).[13] The three peaks were selected in the amide I region with a 25 cm^{-1} band width at half-height. Allowing for homogeneous and heterogeneous broadening, the band fitting was allowed a ±3 cm^{-1} window with respect to each actual band. A mixed Gaussian and Lorentzian function was employed. Two bands at ∼1604 cm^{-1} and ∼1615 cm^{-1}, due to ring modes from the Phe and Tyr side-chains, were included along with amide I bands in the band-fitting procedure. The baseline was taken as a linear function as described.[13] Possible contributions from Asn and Gln side-chains in the amide I region were not taken into account, as they constitute <7% of the amide bonds.

Atomic force microscopy

α-Synuclein solutions were mixed gently prior to removal of aliquots for AFM analysis. The aliquots (1–2 µl) were applied to a freshly cleaved muscovite mica substrate and kept at room temperature for 30 s. The mica surface was then rinsed with Millipore-filtered water (2×50 µl) to remove loosely bound protein and dried under a stream of nitrogen. The sample was imaged immediately using a Nanoscope IV controller (Digital Instruments, Santa Barbara, CA) with a Multimode scanning probe microscope equipped with an E-scanner. All measurements were carried out in the tapping mode under ambient conditions using single-beam silicon cantilever probes.

Native gel electrophoresis

Native (non-denaturing) polyacrylamide gel electrophoresis was performed at a constant 100 V with a Mini–PROTEIN II Bio-Rad electrophoresis system using a Tris–HCl 7.5% (w/v) polyacrylamide gel. The gels were stained with SYPRO Ruby (Molecular Probes) protein gel stain and were visualized by fluorescence under UV light. Approximately 2 ng of protein per band was required for detection when gels were stained with SYPRO Ruby dye.

Thioflavin-T binding

ThT fluorescence measurements were performed on an SLM Aminco spectrofluorimeter, using a 10 mm light-path quartz cuvette. Fluorescence emission spectra were recorded from 465–600 nm with excitation at 446 nm. α-Synuclein solutions (4 µl) were thoroughly mixed with 1 ml of 10 µM ThT in 20 mM sodium phosphate buffer

(pH 7.5), with immediate acquisition of the fluorescence emission spectrum.

References

1. Ross, C. A. & Poirier, M. A. (2004). Protein aggregation and neurodegenerative disease. *Nature Rev. Neurosci.* **10**, S10–S17.
2. Spillantini, M. G., Crowther, R. A., Jakes, R., Hasegawa, M. & Goedert, M. (1998). α-Synuclein filamentous inclusions of Lewy bodies from Parkinson's disease and dementia with Lewy bodies. *Proc. Natl Acad. Sci. USA*, **95**, 6469–6473.
3. Polymeropoulos, M. H., Lavedan, C., Leroy, E., Ide, S. E., Dehejia, A., Dutra, A. *et al.* (1997). Mutation in the α-synuclein gene identified in families with Parkinson's disease. *Science*, **276**, 2045–2047.
4. Kruger, R., Kuhn, W., Muller, T., Woitalla, D., Graeber, M., Kosel, S. *et al.* (1998). Ala30Pro mutation in the gene encoding α-synuclein in Parkinson's disease. *Nature Genet.* **18**, 106–108.
5. Masliah, E., Rockenstein, E., Veinbergs, I., Mallory, M., Hashimoto, M., Takeda, A. *et al.* (2000). Dopaminergic loss and inclusion body formation in α-synuclein mice: Implications for neurodegenerative disorders. *Science*, **287**, 1265–1269.
6. Feany, M. B. & Bender, W. W. (2000). A *Drosophila* model of Parkinson's disease. *Nature*, **404**, 394–398.
7. Conway, K. A., Harper, J. D. & Lansbury, P. T., Jr (2000). Fibrils formed *in vitro* from α-synuclein and two mutant forms linked to Parkinson's disease are typical amyloid. *Biochemistry*, **39**, 2552–2563.
8. Conway, K. A., Lee, S. J., Rochet, J. C., Ding, T. T., Williamson, R. E. & Lansbury, P. T., Jr (2000). Acceleration of oligomerization, not fibrillization, is a shared property of both α-synuclein mutations linked to early-onset Parkinson's disease: implications for pathogenesis and therapy. *Proc. Natl Acad. Sci. USA*, **97**, 571–576.
9. Volles, M. J., Lee, S. J., Rochet, J. C., Shtilerman, M. D., Ding, T. T., Kessler, J. C. & Lansbury, P. T., Jr (2001). Vesicle permeabilization by protofibrillar alpha-synuclein: implications for the pathogenesis and treatment of Parkinson's disease. *Biochemistry*, **40**, 7812–7819.
10. Lashuel, H., Petre, B., Wall, J., Simon, M., Nowak, R., Walz, T. & Lansbury, P. (2002). α-Synuclein especially the Parkinson's disease-associated mutants, forms pore-like annular and tubular protofibrils. *J. Mol. Biol.* **322**, 1089–1102.
11. Caughey, B. & Lansbury, P. T. (2003). Protofibrils, pores, fibrils, and neurodegeneration: separating the responsible protein aggregates from the innocent bystanders. *Annu. Rev. Neurosci.* **26**, 267–298.
12. Goldberg, M. S. & Lansbury, P. T. (2000). Is there a cause-and-effect relationship between α-synuclein fibrillization and Parkinson's disease? *Nature Cell Biol.* **2**, E115–E119.
13. Maiti, N. C., Apetri, M. M., Zagorski, M. G., Carey, P. R. & Anderson, V. E. (2004). Raman spectroscopic characterization of secondary structure in natively unfolded proteins: α-synuclein. *J. Am. Chem. Soc.* **126**, 2399–2408.
14. Eliezer, D., Kutluay, E., Bussell, R., Jr & Browne, G. (2001). Conformational properties of α-synuclein in its free and lipid-associated states. *J. Mol. Biol.* **307**, 1061–1073.
15. Narhi, L., Wood, S. J., Steavenson, S., Jiang, Y., Wu, G. M., Anafi, D. *et al.* (1999). Both familial Parkinson's disease mutations accelerate α-synuclein aggregation. *J. Biol. Chem.* **274**, 9843–9846.
16. Serpell, L. C., Berriman, J., Jakes, R., Goedert, M. & Crowther, R. A. (2000). Fiber diffraction of synthetic α-synuclein filaments shows amyloid-like cross-β conformation. *Proc. Natl Acad. Sci. USA*, **97**, 4897–4902.
17. Eker, F., Griebenow, K. & Schweitzer-Stenner, R. (2004). Aβ(1-28) fragment of the amyloid peptide predominantly adopts a polyproline II conformation in an acidic solution. *Biochemistry*, **43**, 6893–6898.
18. Dong, J., Atwood, C. S., Anderson, V. E., Siedlak, S. L., Smith, M. A., Perry, G. & Carey, P. R. (2003). Metal binding and oxidation of amyloid-beta within isolated senile plaque cores: Raman microscopic evidence. *Biochemistry*, **42**, 2768–2773.
19. Miura, T., Suzuki, K., Kohata, N. & Takeuchi, H. (2000). Metal binding modes of Alzheimer's amyloid beta-peptide in insoluble aggregates and soluble complexes. *Biochemistry*, **39**, 7024–7031.
20. Carey, P. R. & Dong, J. (2004). Following ligand binding and ligand reactions in proteins *via* Raman crystallography. *Biochemistry*, **43**, 8885–8893.
21. Sane, S. U., Cramer, S. M. & Przybycien, T. M. (1999). A holistic approach to protein secondary structure characterization using amide I band Raman spectroscopy. *Anal. Biochem.* **269**, 255–272.
22. Overman, S. A. & Thomas, G. J. (1999). Raman markers of nonaromatic side chains in an α-helix assembly: Ala, Asp, Glu, Gly, Ile, Leu, Lys, Ser, and Val residues of phage fd subunits. *Biochemistry*, **38**, 4018–4027.
23. Harper, J. D., Wong, S. S., Lieber, C. M. & Lansbury, P. T. (1997). Observation of metastable Aβ amyloid protofibrils by atomic force microscopy. *Chem. Biol.* **4**, 119–125.
24. Conway, K. A., Harper, J. D. & Lansbury, P. T. (1998). Accelerated *in vitro* fibril formation by a mutant α-synuclein linked to early-onset Parkinson disease. *Nature Med.* **4**, 1318–1320.
25. Conway, K. A., Lee, S. J., Rochet, J. C., Ding, T. T., Harper, J. D., Williamson, R. E. & Lansbury, P. T., Jr (2000). Accelerated oligomerization by Parkinson's disease linked α-synuclein mutants. *Ann. NY Acad. Sci.* **920**, 42–45.
26. Ding, T. T., Lee, S. J., Rochet, J. C. & Lansbury, P. T. (2002). Annular α-synuclein protofibrils are produced when spherical protofibrils are incubated in solution or bound to brain-derived membranes. *Biochemistry*, **41**, 10209–10217.
27. Jo, E., McLaurin, J., Yip, C. M., St George-Hyslop, P. & Fraser, P. E. (2000). α-Synuclein membrane interactions and lipid specificity. *J. Biol. Chem.* **275**, 34328–34334.
28. Munishkina, L. A., Phelan, C., Uversky, V. N. & Fink, A. L. (2003). Conformational behavior and aggregation of α-synuclein in organic solvents: modeling the effects of membranes. *Biochemistry*, **42**, 2720–2730.
29. Lee, H. J., Choi, C. & Lee, S. J. (2002). Membrane-bound α-synuclein has a high aggregation propensity and the ability to seed the aggregation of the cytosolic form. *J. Biol. Chem.* **277**, 671–678.
30. Lowe, R., Pountney, D. L., Jensen, P. H., Gai, W. P. & Voelcker, N. H. (2004). Calcium (II) selectively induces α-synuclein annular oligomers *via* interaction with the C-terminal domain. *Protein Sci.* **13**, 3245–3252.
31. Bustamante, C. & Keller, D. (1995). Scanning force microscopy in biology. *Phys. Today*, **48**, 32–39.

32. Dong, J., Wan, Z. L., Popov, M., Carey, P. R. & Weiss, M. A. (2003). Insulin assembly damps conformational fluctuations: Raman analysis of amide I linewidths in native states and fibrils. *J. Mol. Biol.* **330**, 431–442.

33. Surewicz, W. K., Mantsch, H. H. & Chapman, D. (1993). Determination of protein secondary structure by Fourier-transform infrared-spectroscopy—a critical-assessment. *Biochemistry,* **32**, 389–394.

34. Miura, T. & Thomas, G. J., Jr (1995). Raman spectroscopy of proteins and their assemblies. *Subcell. Biochem.* **24**, 55–99.

35. Thomas, G. J. (2002). New structural insights from Raman spectroscopy of proteins and their assemblies. *Biopolymers,* **67**, 214–225.

36. Lansbury, P. T. (1999). Evolution of amyloid: What normal protein folding may tell us about fibrillogenesis and disease. *Proc. Natl Acad. Sci. USA,* **96**, 3342–3344.

37. Sunde, M. & Blake, C. C. F. (1998). From the globular to the fibrous state: protein structure and structural conversion in amyloid formation. *Quart. Rev. Biophys.* **31**, 1–39.

38. Sunde, M., Serpell, L. C., Bartlam, M., Fraser, P. E., Pepys, M. B. & Blake, C. C. F. (1997). Common core structure of amyloid fibrils by synchrotron X-ray diffraction. *J. Mol. Biol.* **273**, 729–739.

39. Serpell, L. C., Fraser, P. E. & Sunde, M. (1999). X-ray fiber diffraction of amyloid fibrils. *Methods Enzymol.* **309**, 526–536.

40. Bouchard, M., Zurdo, J., Nettleton, E. J., Dobson, C. M. & Robinson, C. V. (2000). Formation of insulin amyloid fibrils followed by FTIR simultaneously with CD and electron microscopy. *Protein Sci.* **9**, 1960–1967.

41. Balbach, J. J., Ishii, Y., Antzutkin, O. N., Leapman, R. D., Rizzo, N. W., Dyda, F. *et al.* (2000). Amyloid fibril formation by Aβ(16-22), a seven-residue fragment of the Alzheimer's β-amyloid peptide, and structural characterization by solid state NMR. *Biochemistry,* **39**, 13748–13759.

42. Balbach, J. J., Petkova, A. T., Oyler, N. A., Antzutkin, O. N., Gordon, D. J., Meredith, S. C. & Tycko, R. (2002). Supramolecular structure in full-length Alzheimer's β-amyloid fibrils: evidence for a parallel β-sheet organization from solid-state nuclear magnetic resonance. *Biophys. J.* **83**, 1205–1216.

43. Jaroniec, C. P., MacPhee, C. E., Astrof, N. S., Dobson, C. M. & Griffin, R. G. (2002). Molecular conformation of a peptide fragment of transthyretin in an amyloid fibril. *Proc. Natl Acad. Sci. USA,* **99**, 16748–16753.

44. Gordon, D. J., Balbach, J. J., Tycko, R. & Meredith, S. C. (2004). Increasing the amphiphilicity of an amyloidogenic peptide changes the beta-sheet structure in the fibrils from antiparallel to parallel. *Biophys. J.* **86**, 428–434.

45. Petkova, A. T., Leapman, R. D., Guo, Z., Yau, W. M., Mattson, M. P. & Tycko, R. (2005). Self-propagating, molecular-level polymorphism in Alzheimer's β-amyloid fibrils. *Science,* **307**, 262–265.

46. Kirkitadze, M. D., Condron, M. M. & Teplow, D. B. (2001). Identification and characterization of key kinetic intermediates in amyloid β-protein fibrillogenesis. *J. Mol. Biol.* **312**, 1103–1119.

47. Laurents, D. V., Gorman, P. M., Guo, M., Rico, M., Chakrabartty, A. & Bruix, M. (2005). Alzheimer's Abeta40 studied by NMR at low pH reveals that sodium 4,4-dimethyl-4-silapentane-1-sulfonate (DSS) binds and promotes β-ball oligomerization. *J. Biol. Chem.* **280**, 3675–3685.

48. Eakin, C. M., Attenello, F. J., Morgan, C. J. & Miranker, A. D. (2004). Oligomeric assembly of native-like precursors precedes amyloid formation by β-2 microglobulin. *Biochemistry,* **43**, 7808–7815.

49. Chi, Z., Chen, X. G., Holtz, J. S. & Asher, S. A. (1998). UV resonance Raman-selective amide vibrational enhancement: quantitative methodology for determining protein secondary structure. *Biochemistry,* **37**, 2854–2864.

50. Ozdemir, A., Lednev, I. K. & Asher, S. A. (2002). Comparison between UV Raman and circular dichroism detection of short α-helices in bombolitin III. *Biochemistry,* **41**, 1893–1896.

51. Bisaglia, M., Tessari, I., Pinato, L., Bellanda, M., Giraudo, S., Fasano, M. *et al.* (2005). A topological model of the interaction between α-synuclein and sodium dodecyl sulfate micelles. *Biochemistry,* **44**, 329–339.

52. Bussell, R., Jr & Eliezer, D. (2001). Residual structure and dynamics in Parkinson's disease-associated mutants of α-synuclein. *J. Biol. Chem.* **276**, 45996–46003.

53. Dong, J., Wan, Z. L., Chu, Y. C., Nakagawa, S. N., Katsoyannis, P. G., Weiss, M. A. & Carey, P. R. (2001). Isotope-edited Raman spectroscopy of proteins: a general strategy to probe individual peptide bonds with application to insulin. *J. Am. Chem. Soc.* **123**, 7919–7920.

54. Huang, R., Kubelka, J., Barber-Armstrong, W., Silva, R. A., Decatur, S. M. & Keiderling, T. A. (2004). Nature of vibrational coupling in helical peptides: an isotopic labeling study. *J. Am. Chem. Soc.* **126**, 2346–2354.

55. Setnicka, V., Huang, R., Thomas, C. L., Etienne, M. A., Kubelka, J., Hammer, R. P. & Keiderling, T. A. (2005). IR study of cross-strand coupling in a β-hairpin peptide using isotopic labels. *J. Am. Chem. Soc.* **127**, 4992–4993.

56. Brauner, J. W., Flach, C. R. & Mendelsohn, R. (2005). A quantitative reconstruction of the amide I contour in the IR spectra of globular proteins: from structure to spectrum. *J. Am. Chem. Soc.* **127**, 100–109.

57. Epand, R. M., Robinson, K. S., Andrews, M. E. & Epand, R. F. (1989). Dependence of the bilayer to hexagonal phase transition on amphiphile chain length. *Biochemistry,* **28**, 9398–9402.

58. Dong, J., Dinakarpandian, D. & Carey, P. R. (1998). Extending the Raman analysis of biological samples to the 100 micromolar concentration range. *Appl. Spectrosc.* **52**, 1117–1122.

59. Marquardt, D. W. (1963). An algorithm for least-squares estimation of nonlinear parameters. *SIAM J. Appl. Math.* **11**, 431–441.

Edited by P. T. Lansbury